Ultrashort optical-vortex pulse generation in few-cycle regime

Keisaku Yamane,[1,2,*] **Yasunori Toda,**[1,2] **and Ryuji Morita**[1,2]

[1]*Department of Applied Physics, Hokkaido University, Kita-13, Nishi-8, Kita-ku, Sapporo, 060-8628 Japan*

[2]*Japan Science and Technology Agency, CREST, 5, Sanbancho, Chiyoda-ku, Tokyo, 102-0075, Japan*

[*]*k-yamane@eng.hokudai.ac.jp*

Abstract: We generated a 2.3-cycle, 5.9-fs, 56-μJ ultrashort optical-vortex pulse (ranging from $\sim$650 to $\sim$950 nm) in few-cycle regime, by optical parametric amplification. It was performed even by using passive elements (a pair of prisms and chirped mirrors) for chirp compensation. Spectrally-resolved interferograms and intensity profiles showed that the obtained pulses have no spatial or topological-charge dispersion during the amplification process. To the best of our knowledge, it is the first generation of optical-vortex pulses in few-cycle regime. They can be powerful tools for ultrabroadband and/or ultrafast spectroscopy and experiments of high-intensity field physics.

OCIS codes: (320.0320) Ultrafast optics; (260.6042) Singular optics; (080.4865) Optical vortices; (320.7110) Ultrafast nonlinear optics; (320.5520) Pulse compression; (190.4970) Parametric oscillators and amplifiers.

References and links

1. A. Mair, A. Vaziri, G. Weihs, and A. Zeilinger, "Entanglement of the orbital angular momentum states of photons," Nature (London) **412,** 313–316 (2001).
2. T. Omatsu, K. Chujo, K. Miyamoto, M. Okida, K. Nakamura, N. Aoki, and R. Morita, "Metal microneedle fabrication using twisted light with spin," Opt. Express **18,** 17967–17973 (2010).
3. J. E. Curtis, B. A. Koss, and D. G. Grier, "Dynamic holographic optical tweezers," Opt. Commun. **207,** 169–175 (2002).
4. F. Krausz and M. Ivanov, "Attosecond physics," Rev. Mod. Phys. **81,** 163–234 (2009).
5. Y. Tokizane, K. Shimatake, Y. Toda, K. Oka, M. Tsubota, S. Tanda, and R. Morita, "Global evaluation of closed-loop electron dynamics in quasi-one-dimensional conductors using polarization vortices," Opt. Express **17,** 24198–24207 (2009).
6. A. Matos-Abiague and J. Berakdar, "Photoinduced charge currents in mesoscopic rings," Phys. Rev. Lett. **94,** 166801 (2005).
7. G. F. Quinteiro and J. Berakdar, "Electric currents induced by twisted light in Quantum Rings," Opt. Express **17,** 20465–20475 (2009).
8. Y-S. Lee, *Principles of Terahertz Science and Technology* (Springer, Berlin, 2009).
9. V. G. Shvedov, C. Hnatovsky, W. Krolikowski, and A. V. Rode, "Efficient beam converter for the generation of high-power femtosecond vortices," Opt. Lett. **35,** 2660–2662 (2010).
10. S. Shiffler, P. Polynkin, and J. Moloney, "Self-focusing of femtosecond diffraction-resistant vortex beams in water," Opt. Lett. **36,** 3834–3836 (2011).
11. M. W. Beijersbergen, L. Allen, H. E. L. O. van der Veen, and J. P. Woerdman, "Astigmatic laser mode converters and transfer of orbital angular momentum," Opt. Commun. **96,** 123–132 (1993).
12. M. W. Beijersbergen, R. P. C. Coerwinkel, M. Kristensen, and J. P. Woerdman, "Helical-wavefront laser beams produced with a spiral phaseplate," Opt. Commun. **112,** 321–327 (1994).
13. K. Sueda, G. Miyaji, N. Miyanaga, and M. Nakatsuka, "Laguerre-Gaussian beam generated with a multilevel spiral phase plate for high intensity laser pulses," Opt. Express **12,** 3548–3553 (2004).

#170738 - $15.00 USD Received 15 Jun 2012; revised 28 Jul 2012; accepted 29 Jul 2012; published 2 Aug 2012

14. A. V. Volyar and T. A. Fadeeva, "Laguerre-Gaussian beams with complex and real arguments in a uniaxial crystal," Opt. Spectrosc. **101,** 450–457 (2006).
15. I. G. Mariyenko, J. Strohaber, and C. J. G. J. Uiterwaal, "Creation of optical vortices in femtosecond pulses," Opt. Express **13,** 7599–7608 (2005).
16. I. Zeylikovich, H. I. Sztul, V. Kartazaev, T. Le, and R. R. Alfano, "Ultrashort Laguerre-Gaussian pulses with angular and group velocity dispersion compensation," Opt. Lett. **32,** 2025–2027 (2007).
17. Y. Tokizane, K. Oka, and R. Morita, "Supercontinuum optical vortex pulse generation without spatial or topological-charge dispersion," Opt. Express **17,** 14517–14525 (2009).
18. A. M. Siddiqui, G. Cirmi, D. Brida, F. X. Kärtner, and G. Cerullo, "Generation of <7 fs pulses at 800 nm from a blue-pumped optical parametric amplifier at degeneracy," Opt. Lett. **34,** 3592–3594 (2009).
19. J. R. Birge, R. Ell, and F. X. Kärtner, "Two-dimensional spectral shearing interferometry for few-cycle pulse characterization, " Opt. Lett. **31,** 2063–2065 (2006).
20. C. Iaconis and I. A. Walmsley, "Self-referencing spectral interferometry for measuring ultrashort optical pulses," IEEE J. Quantum Electron. **35,** 501–509 (1999).
21. K. Yamane, M. Katayose, and M. Yamashita, "Spectral phase characterization of two-octave bandwidth pulses by two-dimensional spectral shearing interferometry based on noncollinear phase matching with external pulse pair," IEEE Photon. Technol. Lett. **23,** 1130–1132 (2011).
22. F. Verluise, V. Laude, Z. Cheng, Ch. Spielmann, and P. Tournois, "Amplitude and phase control of ultrashort pulses by use of an acousto-optic programmable dispersive filter: pulse compression and shaping," Opt. Lett. **25,** 575–577 (2000).
23. A. M. Weiner, "Femtosecond pulse shaping using spatial light modulators," Rev. Sci. Instrum. **71,** 1929–1960 (2000).
24. K. Yamane, Z. Zhang, K. Oka, R. Morita, M. Yamashita, and A. Suguro, "Optical pulse compression to 3.4fs in the monocycle region by feedback phase compensation," Opt. Lett. **28,** 2258–2260 (2003).

1. Introduction

Optical vortices attract growing attention during last decade because of their unique properties of carrying orbital angular momentum (OAM), possessing a dark hole and a phase singularity in the center. An optical vortex is now expected to be applied to quantum information processing [1], laser ablation [2], optical tweezers [3], etc. The essential property of optical vortex is that the phase distribution varies linearly with the azimuthal angle, which gives us a new controllable parameter of light wave in space domain.

For the generation of optical vortices, (quasi-)continuous wave has been utilized in many cases so far because of interest to their singular properties in space domain. The new light source well-merged with powerful control technique in time or frequency domain such as femtosecond technology enables us to carry out experiments for high-intensity field physics [4], ultrafast nonlinear spectroscopy [5–7], terahertz vortex generation based on radiation from coherently-accelerated charged particles along the azimuthal direction [8]. Recently, optical-vortex light sources by the use of femtosecond pulses were reported [9, 10]. However, fruitful achievement by recent femtosecond technology, such as extremely-short intense pulse generation, optical comb generation, pulse shaping, has not been employed.

The key technology for such a light source is to broaden the bandwidth of the optical-vortex converter. Now there are a variety of ways to generate optical vortices, such as combination of cylindrical lenses [11], a spiral phase plate [12, 13], a computer-generated hologram using liquid crystal spatial light modulator (LC-SLM) [3], and a uniaxial crystal [9, 14]. However most of these devices have serious limitations, particularly in the bandwidth. The cylindrical lenses pose chromatic aberration. The spiral phase plates lead to not only topological-charge dispersion but also azimuthal-angle-dependent group delay, which give rise to unwanted effects especially on generation of few-cycle optical pulses. The programmable hologram by LC-SLM, although allowing us to generate the optical vortices with almost any topological charge, brings about angular dispersion owing the diffraction effect. While the dispersion can be compensated for by using an additional diffraction optics [15], like a compensation of the angular dispersion, this compensation procedure is complicated as well as inherently imperfect; while, in the-

#170738 - $15.00 USD Received 15 Jun 2012; revised 28 Jul 2012; accepted 29 Jul 2012; published 2 Aug 2012

ory, a perfect conversion is possible in a 4-f configuration [16], its throughput is quite limited ($\sim$1%). The optical-vortex conversion using a uniaxial crystal, though enabling to generate the ultrabroadband intense pulses, is constrained by the conservation law of the total angular momentum (quantum number) $j = \ell + s$, where ℓ and s denote topological charge associated with OAM and index of spin angular momentum (SAM), respectively. Left- and right-handed circular polarization corresponds to $s = \pm 1$, respectively.

Recently, we have demonstrated the generation of ultrabroadband optical-vortex pulses ranging from $\sim$500 to $\sim$800 nm by the use of an axially-symmetric polarizer (ASP), one of of photonic crystal plates [17]. The technique is easy-to-use and applicable to ultrabroadband pulses without invoking topological-charge or angular dispersions. In addition, the photonic crystal plate with suitable fine structure allows us to generate optical vortex with any topological charge unconstrained by the above-mentioned conservation law. However, the output was limited to several μJ/cm^2 owing to the low damage threshold of the ASP.

To overcome this issue, we employ optical parametric amplification (OPA) of ultrabroadband optical-vortex pulses with preservation of topological charge. Moreover, the femtosecond technologies of chirp compensation and pulse characterization are applied, enabling us to compress the amplified optical-vortex pulses. In the present paper, we report the first generation of ultrashort optical-vortex pulses in few-cycle regime.

2. Experimental setup and results

Our system consists of the following four blocks: parts for (i) generation of ultrabroadband optical-vortex pulses, (ii) OPA for the seeding optical vortex, (iii) chirp compensation and (iv) pulse characterization. First, we explain our optical-vortex converter for the seeding pulses by Jones matrices. The converter is similar to that in our previous work [17], except using axially-symmetric half-wave plate (ASWP) instead of ASP. Here, the ASWP is composed of 12-segmented parts, the fast-axis direction of which varies linearly with half of azimuthal angle. In our setup, the ASWP is sandwiched between two quarter-wave plates (see Fig. 1). To describe the optical-vortex converter, we introduce the following Jones matrices:

$$Q(\theta) = \frac{\mathrm{i}}{\sqrt{2}} \begin{pmatrix} 1-\mathrm{i}\cos 2\theta & -\mathrm{i}\sin 2\theta \\ -\mathrm{i}\sin 2\theta & 1+\mathrm{i}\cos 2\theta \end{pmatrix}, \tag{1}$$

$$A = \begin{pmatrix} \cos\phi & \sin\phi \\ \sin\phi & -\cos\phi \end{pmatrix} \tag{2}$$

with azimuthal angle ϕ, where $Q(\theta)$ and A are the corresponding Jones matrices of the quarter-wave plate and ASWP, respectively. The fast-axis angle of the quarter-wave plate from the horizontal direction is denoted by θ. The total Jones Matrix T of these 3 wave plates is ex-

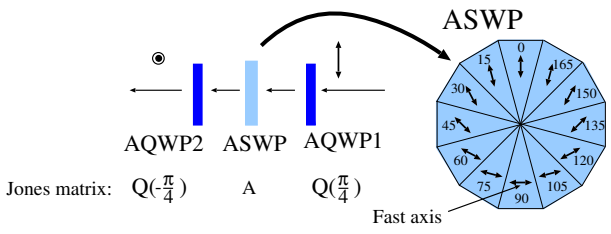

Fig. 1. Optical-vortex converter consisting of an axially-symmetric half-wave plate (ASWP) and achromatic quarter-wave plates (AQWP1, 2).

#170738 - $15.00 USD Received 15 Jun 2012; revised 28 Jul 2012; accepted 29 Jul 2012; published 2 Aug 2012

pressed by

$$T = Q\left(-\frac{\pi}{4}\right)AQ\left(\frac{\pi}{4}\right) = \mathrm{i}\begin{pmatrix} 0 & \mathrm{e}^{\mathrm{i}\phi} \\ -\mathrm{e}^{-\mathrm{i}\phi} & 0 \end{pmatrix}. \quad (3)$$

Equation (3) shows that the system can convert a linearly-polarized beam into an optical vortex with topological charge of $\ell = 1$ or -1. Because axially-symmetric photonic crystal plates have ultrabroad bandwidth [17], the combination with achromatic quarter-wave plates (AQWPs) enables us to convert an ultrabroadband, spatially-Gaussian optical pulse to an ultrabroadband optical vortex, which is used as a seed source for a parametric amplifier. The current configuration using ASWP is superior to that using ASP in the previous report [17], in terms of higher throughput ($\sim$100% vs. $\sim$25%) and lower material dispersion because an additional polarizer is not required. We emphasize that this system gives the output beam only the azimuthal-angle-dependent phase shift, not group delay.

The concept of our OPA system is based on the work by Siddiqui et al [18]. The seeding white light continuum (WLC) is generated by the output from near-infrared (NIR) OPA pumped by fundamental beam from Ti:sapphire amplifier. Unlike WLC generated by fundamental beam itself, the WLC generation by NIR pulses ensures smooth behaviors of spectral phase and intensity around the fundamental wavelength and thus enables us to compensate for the chirp of the seeding pulse by use of only the passive devices such as a prism pair, a grating pair and chirped mirrors. The generated seed pulses are amplified at degeneracy by the second-harmonic of the fundamental beam. The mode mismatch between (nearly Gaussian) pump and (doughnut-like) seed beams reduces the theoretical gain of $\sim$1000 in our OPA to few hundreds. In order to compensate for the reduced gain and get better stability by saturation in the OPA process, we employ a 2-stage OPA scheme. The chirp of the amplified pulses is compensated for by chirped mirrors and characterized by two-dimensional spectral-shearing interferometry (2DSI) [19], which is similar to spectral phase interferometry for direct electric-field reconstruction (SPIDER) [20] and enables to retrieve spectral phase and temporal profile of ultrashort optical pulses. The 2DSI is superior to the SPIDER in that precise measurement of delay time between a pulse pair and a spectrometer with high resolution are not required. The topological charge is observed by a folded self-referenced interferogram [17].

The schematic of the whole experimental setup is shown in Fig. 2. The output from Ti:sapphire laser amplifier (center wavelength λ_c =800 nm, pulse duration: 25 fs, pulse energy: 3.3 mJ, repetition rate: 1 kHz) was sent to a 200 μm-thick β-$BaBO_3$ (BBO) crystal (cut angle θ = 29.2°) to generate pumping pulses (first stage: 50 μJ, second stage: 700 μJ) for a

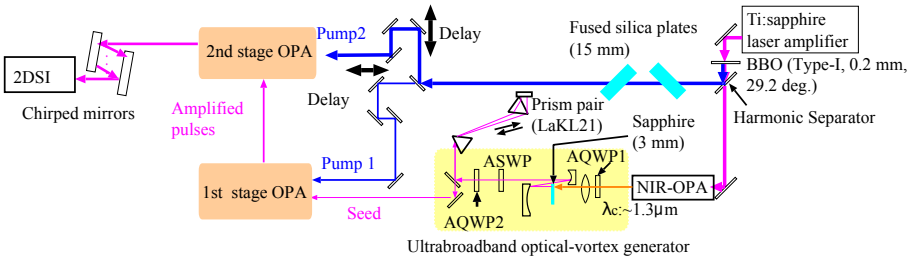

Fig. 2. Schematic of experimental setup for parametric amplification of broadband optical-vortex pulses. AQWP1 and AQWP2: achromatic quarter-wave plates for 1200-1650 nm and 700-1000 nm , respectively.

#170738 - $15.00 USD Received 15 Jun 2012; revised 28 Jul 2012; accepted 29 Jul 2012; published 2 Aug 2012

2-stage OPA by frequency-doubling. The generated second-harmonic and the residual fundamental were separated from each other by a harmonic separator. The former beam (pumping pulse) was temporally-stretched to ∼300 fs by two 15-mm-thick fused silica plates inclined at the Brewster angles. This procedure decreases the peak power of the pump, avoiding pump-induced superfluorescence, and improve the temporal overlapping between the pump and seeding pulses. The latter was sent to a home-built NIR OPA. A small portion of the input fundamental beam to the NIR OPA was focus on a 3-mm-thick *c*-cut sapphire plate to generate the WLC, which was amplified in a 2.4-mm-thick type-II BBO crystal (cut angle θ = 28°) by the unused portion (∼100 μJ) of the fundamental. A portion (∼1 μJ, λ_c =∼1.3 μm) of the output from the NIR OPA was converted to a circularly-polarized beam by an AQWP (1200–1650nm, retardance error: within ± 2% from 1200 to 1650 nm) before WLC generation, not after it (see ultrabroadband optical-vortex generator in Fig. 2). This layout of polarization conversion at ∼1.3 μm can decrease the influence of material dispersion in comparison with in the latter case because glass used in a typical AQWP has zero-dispersion around ∼1.2–∼1.4 μm. The circularly-polarized NIR pulses were focused on a 3-mm-thick *c*-cut sapphire plate and thus the generated circularly-polarized WLC beam passed through the ASWP (λ_c = 808 nm, retardance of π, Photonic Lattice Inc.) and another AQWP (∼700–∼1000 nm, retardance error: within ± 4% from 650 to 1000 nm). To evaluate the topological charge, measurement of the folded self-referenced interferograms [17] was employed. It is based on the interference between identical two optical vortices, except for their signs of the topological charges. As a result, the number of branches in a forked dislocation equal to $|\ell - (-\ell)| = 2|\ell|$. As shown in Fig. 3, the interferograms with 2-pronged dislocations showed that the resulting seed was co-centered ultrabroadband optical-vortex beam with a topological charge of ℓ = 1. In addition, it indicates that the ASWP works well in this ultrabroadband wavelength region ranging from ∼650 to ∼950 nm.

A Brewster-cut prism pair (material: LaKL21) was employed to decrease the positive 3rd-order dispersion (the difference between with and without the prism pair will be described in the pulse characterization results). After passing through it, the seeding vortex pulses were temporally and spatially overlapped with the pumping pulses at small angles (∼1°) in the 2 OPA stages. The 1-mm-thick BBO crystals (cut angle θ = 40°) were utilized as gain media in both the stages, and the angles of the crystals were carefully tuned to get the broadest gain around at the degeneracy [18]. The seeding pulses were boosted up to ∼1 μJ and ∼ 70 μJ in the 1st and 2nd stages, respectively. After the chirp of the amplified pulses was compensated for by chirped mirrors (∼-25 fs^2/bounce, 500-1000 nm), the spectral phase was measured by a

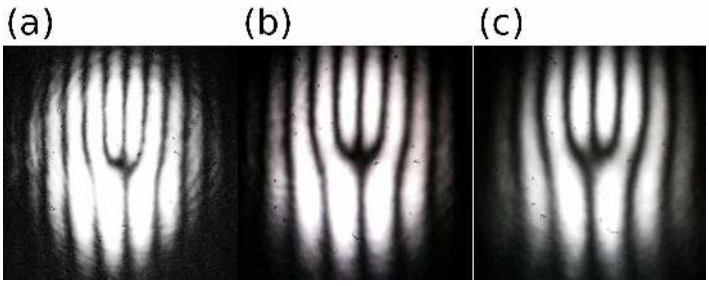

Fig. 3. Spectrally-resolved, folded self-referenced interferograms (co-centered interferograms between ℓ=±1 beams) of seeding optical-vortex pulses after band-pass filtering at the center wavelengths of (a) 650, (b) 800 and (c) 950 nm.

#170738 - $15.00 USD Received 15 Jun 2012; revised 28 Jul 2012; accepted 29 Jul 2012; published 2 Aug 2012

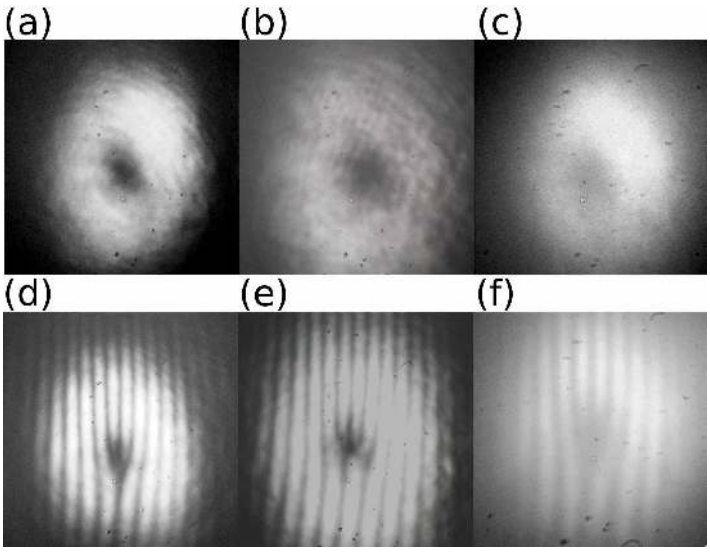

Fig. 4. (a)-(c) Beam profiles and (d)-(e) folded self-referenced interferograms (co-centered interferograms between ℓ=$\pm$1 beams) of amplified optical-vortex pulses after band-pass filtering at the center wavelengths of 650 ((a) and (d)), 800 ((b) and (e)) and 950 nm ((c) and (f)).

home-built 2DSI apparatus [21].

Figure 4 shows the beam profiles and the folded self-referenced interferograms (co-centered interferograms between ℓ=$\pm$1 beams) of the amplified beam. The beam diameter of the output was $\sim$5 mm. The beam profiles are co-centered doughnut-like over the entire bandwidth; the self-referenced interferograms indicate that the initial topological charge ($\ell = 1$) of seeding pulses was conserved in the amplification process. Figures 3 and 4 indicate that our optical-vortex converter works well in ultrabroadband region (from $\sim$650 to $\sim$950 nm). Even if the ASWP has non-negligible retardance error, it does not cause a serious issue in our configuration. This is because the prism pair and the phase-matched OPA process select only a favorable component with horizontal polarization, eliminating other polarization components. Therefore, the influence by the retardance error is negligible in our configuration.

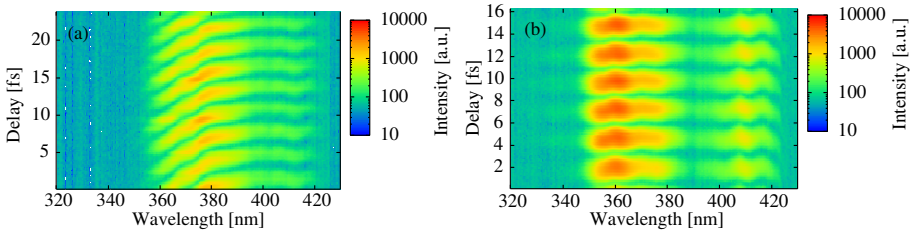

Fig. 5. The interferograms of the generated ultrabroadband optical-vortex pulses after parametric amplification and chirp compensation (a) without and (b) with prism pair. They were measured by 2DSI under the following conditions: spectral shear; (a) 65 rad/ps, (b) 22 rad/ps, spectral shift by chirped reference pulses; (a) 2.35 rad/fs, (b) 2.46 rad/fs.

The measured 2DSI interferogram , which were upconverted by sum-frequency mixing with

#170738 - $15.00 USD Received 15 Jun 2012; revised 28 Jul 2012; accepted 29 Jul 2012; published 2 Aug 2012

strongly chirped pulses, are shown in Fig. 5. The number of delay points and the accumulation time for each spectrum in our 2DSI were 128 and 20 ms, respectively. The reconstruction of the spectral phase was completed within ∼5 s including measurement time. The interferograms were very clear in the entire wavelength regions and stable within the measurement time. First, only the chirped mirrors (10 bounces) without the LaKL21 prism pair (see Fig. 2) was employed to roughly estimate the residual dispersion. Figure 5(a) shows that quadratic behaviors in the interferogram still remained, which reflected the existence of non-negligible positive 3rd order dispersion (∼1000 fs^3). In order to reduce the residual chirp, we put the prism pair for pre-chirp-compensation and adjusted the distance between the prisms and the number of the bounces of the amplified beam at the chirped mirrors. As a result, the distance of 37 cm and 10 bounces minimized the residual chirp, yielding the compressed pulse energy of 56 μJ. The very flat behavior of the interferogram implies that the chirp was almost compensated for (see Fig. 5(b)). The retrieved phase, together with the measured spectrum of the amplified pulses, is shown in Fig. 6(a). Owing to smooth behavior of the spectral phase in the entire wavelength region, which was ascribed to the WLC generation from the NIR pulses, the chirp of the generated pulses was almost compensated for by using only prism pair and chirped mirrors. This compensation was performed even without any help of active chirp compensator such as an acousto-optic dispersive filter [22] or a 4-f pulse shaper with an LC-SLM [23, 24]. The pulse duration of the reconstructed temporal intensity profile was 5.9 fs (see Fig. 6(b)), which was close to that (5.5 fs) of the corresponding Fourier transform-limited pulse. The cycle number of the reconstructed pulse was 2.3 (center wavelength $\lambda_c = 763$ nm). To the best of our knowledge, this is the first generation of ultrashort optical-vortex pulses in the few-cycle regime.

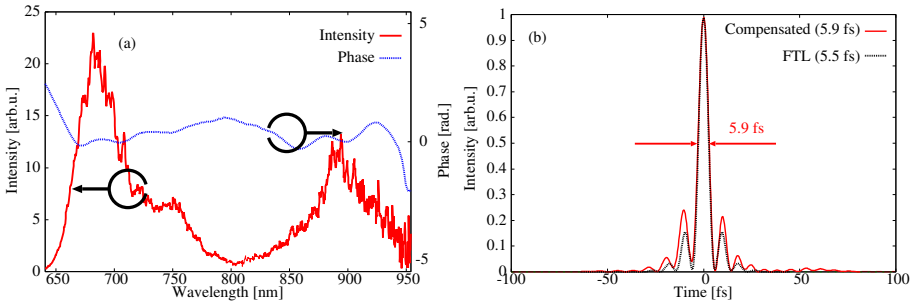

Fig. 6. (a) Measured spectral intensity and retrieved spectral phase of the generated ultrashort optical-vortex pulses. (b) The temporal profile of the reconstructed pulse, together with that of the corresponding Fourier-transform-limited pulse.

3. Conclusion

We generated a 5.9-fs, 56-μJ, 2.3-cycle ultrashort optical-vortex pulses (ranging from ∼650 to ∼950 nm) in few-cycle regime, even by using only passive chirp-compensation elements (a prism pair and chirped mirrors). The result was achieved by the broadband optical-vortex generation technique well-merged with recent progressing ultrafast technologies. In our scheme, an ultrabroadband vortex pulse was amplified through the first and second optical parametric processes at degeneracy. The spectrally-resolved self-referenced interferograms and intensity profiles indicated that obtained ultrashort optical-vortex pulses in few-cycle regime have no spatial or topological-charge dispersion.

The great advantage of an OPA technique is its power scalability. The application of recent optical parametric chirped-pulse amplification (OPCPA) technique will enable us to generate

#170738 - $15.00 USD Received 15 Jun 2012; revised 28 Jul 2012; accepted 29 Jul 2012; published 2 Aug 2012

mJ-level high-power ultrashort optical-vortex pulses, which will open a new world of ultrafast, ultrabroadband and high-intensity singular optics.

Acknowledgments

This work was partially supported by Grant-in-Aids for Scientific Research (B) (No. 23360024, 2011-2014) and Exploratory Research (No. 23656040, 2011-2013) from Japan Society for the Promotion of Science (JSPS).

#170738 - $15.00 USD Received 15 Jun 2012; revised 28 Jul 2012; accepted 29 Jul 2012; published 2 Aug 2012